

This discussion paper is/has been under review for the journal Hydrology and Earth System Sciences (HESS). Please refer to the corresponding final paper in HESS if available.

The impact of land surface temperature on soil moisture anomaly detection from passive microwave observations

R. M. Parinussa^{1,2}, T. R. H. Holmes¹, and W. T. Crow¹

¹USDA ARS Hydrology and Remote Sensing Laboratory, Beltsville, MD, USA

²Department of Hydrology and Geo-environmental Sciences, Faculty of Earth and Life Sciences, VU University Amsterdam, Amsterdam, The Netherlands

Received: 5 July 2011 – Accepted: 7 July 2011 – Published: 11 July 2011

Correspondence to: R. M. Parinussa (robert.parinussa@falw.vu.nl)

Published by Copernicus Publications on behalf of the European Geosciences Union.

HESSD

8, 6683–6719, 2011

The impact of land surface temperature on soil moisture anomaly detection

R. M. Parinussa et al.

Title Page

Abstract

Introduction

Conclusions

References

Tables

Figures

⏪

⏩

◀

▶

Back

Close

Full Screen / Esc

Printer-friendly Version

Interactive Discussion

Abstract

For several years passive microwave observations have been used to retrieve soil moisture from the Earth's surface. Low frequency observations have the most sensitivity to soil moisture, therefore the modern Soil Moisture and Ocean Salinity (SMOS) and future Soil Moisture Active and Passive (SMAP) satellite missions observe the Earth's surface in the L-band frequency. In the past, several satellite sensors such as the Advanced Microwave Scanning Radiometer-EOS (AMSR-E) and Windsat have been used to retrieve surface soil moisture using multi-channel observations obtained at higher microwave frequencies. While AMSR-E and Windsat lack an L-band channel, they are able to leverage multi-channel microwave observations to estimate additional land surface parameters. In particular, the availability of Ka-band observations allows AMSR-E and Windsat to obtain surface temperature estimates required for the retrieval of surface soil moisture. In contrast, SMOS and SMAP carry only a single frequency radiometer. Because of this, ancillary – and potentially less accurate – sources of surface temperature information (e.g. re-analysis data from operational weather prediction centers) must be sought to produce surface soil moisture retrievals. Here, two newly-developed, large-scale soil moisture evaluation techniques, the triple collocation (TC) approach and the R_{value} data assimilation approach, are applied to quantify the global-scale impact of replacing Ka-band based surface temperature retrievals with Modern Era Retrospective-analysis for Research and Applications (MERRA) surface temperature predictions on the accuracy of Windsat and AMSR-E surface soil moisture retrievals. Results demonstrate that under sparsely vegetated conditions, the use of Ka-band radiometric land surface temperature leads to better soil moisture anomaly estimates compared to those retrieved using MERRA land surface temperature predictions. However the situation is reversed for highly vegetated conditions where soil moisture anomaly estimates retrieved using MERRA land surface temperature are superior. In addition, the surface temperature phase shifting approach is shown to generally enhance the value of MERRA surface temperature estimates for soil moisture retrieval.

The impact of land surface temperature on soil moisture anomaly detection

R. M. Parinussa et al.

Title Page

Abstract

Introduction

Conclusions

References

Tables

Figures



Back

Close

Full Screen / Esc

Printer-friendly Version

Interactive Discussion



techniques have been proposed with circumvent the need for extensive ground-based soil moisture observations.

The first technique was introduced by Crow et al. (2007) and is based on calculating the Pearson correlation coefficient (R_{value}) between rainfall errors and Kalman filter analysis increments realized during the assimilation of remotely sensed soil moisture products into an antecedent precipitation index (API). Recently, Crow et al. (2010) adapted this method to run on an anomaly basis and by calculating API analysis increments using a Rauch-Tung-Striebel smoother instead of a Kalman filter.

The second evaluation technique is based on a so-called Triple Collocation (TC) analysis which was first applied to soil moisture observations by Scipal et al. (2008). TC is a powerful statistical tool for estimating root mean square error (RMSE) in a time series of geophysical data by simultaneously solving for systematic differences in the climatology of a set of three linearly related data sources with independent error structures. Recently, Miralles et al. (2010) validated the TC technique with in situ soil moisture data from four heavily instrumented watersheds located in the United States and Dorigo et al. (2010) used this technique to rank the quality of different soil moisture products.

Our analysis is based on the application of both the TC and R_{value} verification techniques to globally evaluate the impact of changing between Ka-band and MERRA-based LST products on the anomaly detection accuracy of subsequent LPRM-based AMSR-E and Windsat soil moisture retrievals. The use of both TC and R_{value} metrics allows for the cross-verification of key results and the first attempt at comparing results from both metrics on a global scale. It also allows for an initial global evaluation of various pre-processing strategies for re-analysis based LST products. Recently, Holmes et al. (2011) argued that time-lagged pre-processing of the MERRA LST observations can improve their accuracy as a representation of the temperature for surface soil moisture retrieval algorithms. Their approach is based on synchronizing temperature observations via the introduction of a phase shift to temperature observations at different depths. This phase shift may vary with land cover and surface state, since

The impact of land surface temperature on soil moisture anomaly detection

R. M. Parinussa et al.

Title Page

Abstract

Introduction

Conclusions

References

Tables

Figures



Back

Close

Full Screen / Esc

Printer-friendly Version

Interactive Discussion



these properties determine the propagation of heat through deeper soil layers. In evaluating several scenarios, based on this phase shift, we hope to better understand errors in SMOS and SMAP soil moisture retrievals associated with the use of non-satellite-based temperature estimates. Also, potential time-lagged pre-processing of the MERRA LST predictions following Holmes et al. (2011) will be evaluated to determine the potential use of phase shifting approaches to enhance the utility of LST products obtained from an atmospheric re-analysis system.

2 Data

2.1 Passive microwave observations

The Advanced Microwave Scanning Radiometer for Earth Observing System (AMSR-E) is a radiometer on board NASA's Aqua satellite which was launched on 4 May 2002. The satellite orbits the Earth at an altitude of 705 km and scans with an incidence angle of 55° . Observations are made in vertical and horizontal polarization at six frequencies, three of which are relevant for this study – 6.9 GHz (C-band), 10.7 GHz (X-band) and 37 GHz (Ka-band). The spatial resolution of the C-, X- and Ka-band observations are 73×43 km, 51×30 km and 14×8 km, respectively. The design of the WindSat radiometer, on board the Coriolis satellite which was launched on 6 January 2003, is based on AMSR-E and has only small changes in specifications (e.g. frequency, bandwidth, incidence angle and calibration procedure). Recently, Parinussa et al. (2011) showed that soil moisture retrievals from both satellites are of similar quality when compared to in situ data after the implementation of an inter-calibration procedure and consistent use of the LPRM retrieval algorithm. The WindSat satellite orbits the Earth at an altitude of 840 km and scans with an incidence angle of 53.5° , 49.9° and 53.0° for C-, X- and Ka-band, respectively.

An important difference between AMSR-E and WindSat is the reduced temporal frequency of WindSat observations as a result of the reduced swath width. Another

The impact of land surface temperature on soil moisture anomaly detection

R. M. Parinussa et al.

Title Page

Abstract

Introduction

Conclusions

References

Tables

Figures



Back

Close

Full Screen / Esc

Printer-friendly Version

Interactive Discussion



5 difference is the local equator overpass times, which are 06:00 a.m./p.m. for the Coriolis satellite (identical to SMOS and SMAP) and 01.30 a.m./p.m. for the Aqua satellite. These differences motivate the use of both WindSat and AMSR-E retrievals in this analysis. In particular, the 06:00 a.m./p.m. overpass time of Windsat matches SMOS and SMAP. This is critical since at the 06:00 a.m./p.m. overpass times of the Coriolis satellite, the soil temperature profile is considered to be more vertically homogeneous than at the 01:30 a.m./p.m. overpass times of the Aqua satellite. However, since the reduced temporal frequency of WindSat observations may introduce higher levels of sampling error in evaluation results, we have also included the AMSR-E results in the analysis. Moreover, the physical conditions of the observed surface are significantly different for the day- (ascending) and night-time (descending) overpass, and are therefore separated in the analysis.

10 Radio frequency interference (RFI) disturbs the natural microwave emission in the C-band frequency over significantly large areas over the United States, India and Japan. The RFI algorithm developed by Li et al. (2004) was used to detect these areas for both satellites. If RFI was detected on a specific location we switched back to observations in the somewhat higher X-band frequency (Fig. 1) for the entire analysis period. For more detailed information on the Aqua AMSR-E sensor and Coriolis WindSat sensor, readers are directed to NSIDC (2006) and Gaiser et al. (2004), respectively.

20 2.2 MERRA data

The Modern Era Retrospective-analysis for Research and Applications (MERRA) is a multi-decadal (30 + years) continuous re-analysis data record developed to support NASA's Earth science objectives (Rienecker et al., 2011). MERRA provides the science and application communities with global analysis with an emphasis on improved estimates of the global hydrological cycle. Three dimensional diagnostics are produced at a 6-hourly interval, while two dimensional diagnostics (including LST) are produced at an hourly interval. This high temporal interval was the main driver of using MERRA LST in this analysis. MERRA data products are coarse scale, having a

The impact of land surface temperature on soil moisture anomaly detection

R. M. Parinussa et al.

Title Page

Abstract

Introduction

Conclusions

References

Tables

Figures



Back

Close

Full Screen / Esc

Printer-friendly Version

Interactive Discussion



spatial resolution of $1/2^\circ$ latitude by $2/3^\circ$ longitude. In this study, MERRA LST data are downscaled to $1/2^\circ$ latitude by $1/2^\circ$ longitude using nearest neighbour re-sampling and observation times were matched with the average $1/2^\circ$ observation times of the satellites.

5 The MERRA surface temperature product was analysed by Holmes et al. (2011), with the focus on the implementation for soil moisture retrievals. In order to account for possible differences between the depth of MERRA's surface layer and the shallow temperature sensing depth for C- and X-band, several scenarios of the MERRA re-analysis products will be evaluated that reflect slightly different soil depths. MERRA
10 data is publically available through the Goddard Earth Sciences Data and Information Services Centre <http://disc.sci.gsfc.nasa.gov/mdisc/data-holdings> for more information on the MERRA data, readers are directed to <http://gmao.gsfc.nasa.gov/merra>.

2.3 Precipitation data

Two separate satellite based rainfall datasets produced by Tropical Rainfall Measuring Mission (TRMM) Multi-satellite Precipitation Analysis (TMPA; Huffman et al., 2007) are also utilized. P^{sat} is based on the real-time TRMM 3B42RT product calculated by combining passive microwave with microwave calibrated infrared satellite data derived from different sensors (Huffman et al., 2007). P^{gauge} is based on the same satellite
15 input data (TRMM 3B42) but includes a retrospective correction based on monthly rain gauge data and is therefore of higher quality than P^{sat} . Both precipitation products are produced quasi-globally (50°N – 50°S) at a 3-hourly interval having a spatial resolution of $1/4^\circ$. In this study, precipitation data was upscaled to $1/2^\circ$ latitude by $1/2^\circ$
20 longitude using spatial averaging and daily representations were generated by accumulating each precipitation product over a 24-h period.

The impact of land surface temperature on soil moisture anomaly detection

R. M. Parinussa et al.

Title Page

Abstract

Introduction

Conclusions

References

Tables

Figures



Back

Close

Full Screen / Esc

Printer-friendly Version

Interactive Discussion

2.4 Scatterometer data

The Advanced Scatterometer (ASCAT) on board ESA's MetOp satellite is an active (radar) instrument operating in the C-band frequency (5.255 GHz) making observations since October 2006. Backscatter measurements at six different azimuth angles are converted to surface soil moisture (SSM) estimates by applying the TU Wien soil moisture change detection algorithm (Naemi et al., 2009). The surface soil moisture value is a relative measure of soil moisture ($\sim 1\text{--}2$ cm) ranging between wilting point and saturation. By the time of the analysis, the product was available from January 2007 till September 2010 and is produced in time series with a spatial resolution of 25 km. In this study, the ascending and descending swaths are combined, which leads to a nearly daily revisit frequency at the equator. Surface soil moisture data was upscaled to $1/2^\circ$ latitude by $1/2^\circ$ longitude using spatial averaging.

2.5 Data selection

Due to differences in availability and characteristics (temporal and spatial resolution) of each dataset, some compromises had to be made. By definition, the triple collocation (TC) method requires 3 independent data sources for the same geophysical variable (Sect. 3.1.2), which restricts the TC analysis to the time period of ASCAT availability between January 2007 and September 2010. The time period for which the datasets required for the R_{value} method are available is significantly longer, from February 2003 till December 2010. This period was chosen to make the analysis periods of the two radiometers (AMSR-E and WindSat) identical.

The spatial resolution of the different datasets range from the highest resolution for the ASCAT data (25 km) to the lowest resolution for the MERRA re-analysis LST product ($1/2^\circ$ latitude by $2/3^\circ$ longitude). The spatial resolution of the passive microwave observations are typically available at $1/4^\circ$ resolution. Also, the different datasets vary in their temporal resolution ranging from the highest resolution for the MERRA re-analysis (global hourly interval) to the lowest resolution for the (active and passive)

HESSD

8, 6683–6719, 2011

The impact of land surface temperature on soil moisture anomaly detection

R. M. Parinussa et al.

Title Page

Abstract

Introduction

Conclusions

References

Tables

Figures

⏪

⏩

◀

▶

Back

Close

Full Screen / Esc

Printer-friendly Version

Interactive Discussion



The impact of land surface temperature on soil moisture anomaly detection

R. M. Parinussa et al.

Title Page

Abstract

Introduction

Conclusions

References

Tables

Figures

⏪

⏩

◀

▶

Back

Close

Full Screen / Esc

Printer-friendly Version

Interactive Discussion

microwave observation. To balance the differences in spatial and temporal availability of the datasets, the entire analysis was executed quasi-globally (50° N–50° S) on a daily timescale for a 1/2° spatial resolution. Moreover, the brightness temperatures from AMSR-E and WindSat were re-sampled to daily 1/2° global grids and day- (ascending), and night (descending) time observations were analysed separate.

The results from the evaluation techniques were analysed over 6 different land cover classes in order to categorize results according to vegetation density. The LPRM retrieves vegetation optical depth, simultaneously with the soil moisture retrievals. Daily LPRM vegetation optical depth retrievals from the night-time AMSR-E overpasses were averaged for the period February 2003 till December 2010 (Fig. 2). Based on this map, the global area over which the analyses were executed (50° N–50° S) is divided into 6 different classes (Table 1; Fig. 3). In the standard LPRM routine it is assumed that the soil moisture signal becomes entirely masked due to the overlying canopy when the simultaneously retrieved vegetation optical depth in the C-band frequency exceeds a value of 0.80. Although the LPRM rejects soil moisture retrievals in these areas on a regular basis, they are considered in this analysis in order to inter-compare TC and R_{value} results over the widest possible range of land surface conditions. Only frozen surfaces are completely removed from the analysis. For areas with detected Radio Frequency Interference, soil moisture retrievals are derived from X-band brightness temperature observations.

Both evaluation techniques require anomaly data which was calculated by decomposing the raw time series data into climatology and anomaly components. For a general geophysical variable A , this decomposition can be represented as

$$\hat{A}_i = A_i - \bar{A}_{\text{DOY}} \quad (1)$$

where \bar{A}_{DOY} is the climatological expectation of a geophysical variable from the entire analysis period, calculated using a 31-day moving window centred on a particular day of the year (DOY), and \hat{A}_i are anomalies relative to these expectations experienced on a particular day i . Prior to the application of either the TC or R_{value} metrics, all soil

moisture and precipitation inputs were decomposed into anomalies following Eq. (1). As a result, this analysis will focus solely on evaluating the accuracy of soil moisture anomaly predictions relative to a fixed climatology. Finally, to allow for direct comparisons between the different scenarios for the LPRM, a particular $1/2^\circ$ grid for a given overpass time is only included in the analysis if it contains a viable retrieval in all evaluated scenarios.

3 Methodology

3.1 Evaluation techniques

3.1.1 R_{value} method

The R_{value} method was introduced by Crow et al. (2007) and is a technique based on calculating the Pearson correlation coefficient (R_{value}) between known rainfall errors and Kalman filter analysis increments realized during the assimilation of remotely sensed soil moisture products into the antecedent precipitation index (API). Typical R_{value} magnitudes range from about 0 to 0.7, where a higher R_{value} indicates high-quality soil moisture retrieval and increased efficiency in the filtering of errors in the API predictions resulting from random error in the satellite-base precipitation product (P^{sat}) used to generate API. Such errors are assumed known once the lower-quality rainfall products P^{sat} , typically obtained from a real-time precipitation dataset, is retrospectively corrected using rain gauge data, resulting in a higher quality precipitation dataset P^{gauge} . Consequently, soil moisture errors can be explicitly calculated as $P^{\text{sat}} - P^{\text{gauge}}$. The overall approach is based on the rationale that the correlation between random rainfall errors and filter correction should increase as the accuracy of the assimilated soil moisture measurements increases.

The impact of land surface temperature on soil moisture anomaly detection

R. M. Parinussa et al.

Title Page

Abstract

Introduction

Conclusions

References

Tables

Figures

⏪

⏩

◀

▶

Back

Close

Full Screen / Esc

Printer-friendly Version

Interactive Discussion

Recently, Crow et al. (2010) adapted the R_{value} approach to run on an anomaly basis (i.e. after precipitation and soil moisture products have been decomposed by Eq. 1 into anomaly components). In this case, API anomalies are defined as

$$\hat{\text{API}}_i = \gamma \cdot \hat{\text{API}}_{i-1} + \hat{P}_i \quad (2)$$

on a day i and γ is assumed equal to a globally constant value of 0.85. Analysis increments are then obtained by assimilating soil moisture anomalies using a Rauch-Tung-Striebel smoother and R_{value} is defined as the sampled correlation coefficient between 5-day moving averages of these analysis increments and 5-day moving averages of error in \hat{P}_i .

Crow et al. (2010) verified this approach using three heavily-instrumented watersheds located in the United States. R_{value} was calculated for a number of different AMSR-E soil moisture products over each site and compared to the correlation coefficient calculated between each product and extensive ground-based soil moisture observations. Results from these comparisons demonstrated that R_{value} accurately captures the anomaly correlation-based skill of soil moisture retrievals without reliance on ground-based soil moisture observations. As an example, the application of R_{value} to the LPRM AMSR-E (descending) soil moisture retrievals product is shown in Fig. 4.

3.1.2 Triple collocation

TC is a statistical tool for estimating root mean square error (RMSE) in time series based on analyzing three linearly related data sources with independent error structure. The approach has been proposed as a potential tool for the validation of remotely sensed surface soil moisture retrievals (Scipal et al., 2008). Miralles et al. (2010) used remotely sensed-, land surface modelled- and in situ soil moisture to estimate the magnitude of point-to-footprint upscaling error for ground-based surface soil moisture observations. Dorigo et al. (2010) used remotely sensed soil moisture from 2 different (active and passive) satellite platforms and re-analysis soil moisture as the third independent data product, to rank the different satellite observed soil moisture products.

The impact of land surface temperature on soil moisture anomaly detection

R. M. Parinussa et al.

Title Page

Abstract

Introduction

Conclusions

References

Tables

Figures



Back

Close

Full Screen / Esc

Printer-friendly Version

Interactive Discussion



Both papers used several combinations (different re-analysis or modelled data) for the third independent data product, and showed that the error estimates are only marginally influenced by the choice of this third dataset.

This paper aims to examine the relative quality of soil moisture products generated by a single retrieval algorithm. For this reason, two soil moisture data sources (API calculated from P^{gauge} and ASCAT) are fixed, while the other product (soil moisture from the LPRM) is evaluated for varying scenarios. All three soil moisture datasets (i.e. θ_{ASCAT} , θ_{API} , and various scenarios of θ_{LPRM}) are decomposed into anomalies using Eq. (1) and both the resulting time series of θ_{API} , and θ_{LPRM} ($\hat{\theta}_{\text{API}}$ and $\hat{\theta}_{\text{LPRM}}$) are rescaled so that they have the same temporal standard deviation as $\hat{\theta}_{\text{ASCAT}}$. The choice of $\hat{\theta}_{\text{ASCAT}}$ as the reference data set is arbitrary and will not affect subsequent manuscript conclusions. Nevertheless, all subsequent RMSE values will be expressed in the dynamic range of $\hat{\theta}_{\text{ASCAT}}$. Following this decomposition Eq. (1) and re-normalization, the RMSE of anomalies in $\hat{\theta}_{\text{LPRM}}$ can be estimated as

$$\text{RMSE}(\hat{\theta}_{\text{LPRM}}) = \left\langle \left(\hat{\theta}_{\text{ASCAT}} - \hat{\theta}_{\text{LPRM}} \right) \left(\hat{\theta}_{\text{LPRM}} - \hat{\theta}_{\text{API}} \right) \right\rangle \quad (3)$$

where the outside angled brackets indicate temporal averaging. The accuracy of Eq. (3) relies on two key theoretical prerequisites of TC being met. First, TC requires a sufficiently large sample (>100) of common observations available for temporal averaging. Second, the most important, TC requires that errors in each of three datasets are substantially uncorrelated. The latter prerequisite is difficult to fulfill (Scipal et al., 2008; Miralles et al., 2010; Dorigo et al., 2010) for soil moisture estimates obtained from complex land surface models and reanalysis systems since such approaches tend to integrate information from a wide, variety of sources. As a result, here we follow Crow et al. (2010) and apply TC to soil moisture estimates obtained from a simple API modeling approach driven only by TMPA precipitation products (P^{gauge}). Miralles et al. (2010) examined the impact of replacing soil moisture estimates from a highly-complex land surface model with a simple API dataset and found that both choices lead to essentially similar TC results. Additionally, the use of a simple API model, instead of a

The impact of land surface temperature on soil moisture anomaly detection

R. M. Parinussa et al.

Title Page

Abstract

Introduction

Conclusions

References

Tables

Figures



Back

Close

Full Screen / Esc

Printer-friendly Version

Interactive Discussion



re-analysis soil moisture product, for the third independent product minimizes possible cross-correlation when replacing Ka-band LST by MERRA re-analysis LST data. As an example, the application of TC to the LPRM AMSR-E (descending) soil moisture retrievals product is shown in Fig. 5.

5 While both the R_{value} and TC verification techniques have been successfully applied in previous soil moisture evaluation studies (Crow et al., 2007, 2010; Scipal et al., 2008; Dorigo et al., 2010), their results have never been inter-compared and neither metric has achieved sufficient independent credibility to serve as true replacement for ground-based soil moisture measurements. For TC-based approaches, the primary concern is
10 the potential for unreliable results for the case of cross-correlated errors (Scipal et al., 2008; Crow et al., 2010). For R_{value} , the analogous concern is ambiguity introduced by the uncertain choice of γ in Eq. (2) and the potential confounding impact of auto-correlated soil moisture retrieval error (Crow et al., 2007). Here we present both R_{value} and TC results in an attempt to enhance the credibility of our global evaluation results
15 by seeking results supported independently by both metrics.

3.2 Land surface temperature scenarios

The analysis in this paper will focus on the application of the TC and R_{value} verification techniques to AMSR-E and Windsat surface soil moisture retrievals generated using a variety of scenarios for parameterizing LST. The first step of these scenarios will
20 be based on the synthetic degradation of LST retrievals from Ka-band measurements (Sect. 3.2.1). This degradation will be used to assess the sensitivity of LPRM surface soil moisture retrievals to LST error, and evaluating the ability of both TC and R_{value} to detect the degrading impact of this error on surface soil moisture retrievals. The second set of scenarios will be based on temperature estimates acquired from MERRA.
25 In order to examine issues related to the vertical support of MERRA temperature observations, several scenarios will be constructed utilizing various phase and amplitude pre-processing modifications to the MERRA surface temperature dataset (Holmes et al., 2011).

The impact of land surface temperature on soil moisture anomaly detection

R. M. Parinussa et al.

Title Page

Abstract

Introduction

Conclusions

References

Tables

Figures



Back

Close

Full Screen / Esc

Printer-friendly Version

Interactive Discussion



3.2.1 Ka-band scenarios

LST is considered to be a critical input parameter to retrieve soil moisture and several algorithms use a method developed by Holmes et al. (2009) to retrieve this parameter. This method is based on a simple linear relation between coincidentally observed vertical polarized Ka-band brightness temperature and the temperature of the land surface, referred to as T_{Ka} . In this paper the Ka-band brightness temperature signal is degraded synthetically by adding a mean-zero, Gaussian random noise signal (uncorrelated in both time and space) to original Ka-band LST retrievals. Here, standard deviations of 0.5, 1, 2 and 4 K are used for these synthetic random perturbations.

3.2.2 MERRA scenarios

The LST from the MERRA re-analysis data set, referred to as T_{MERRA} , represents a much shallower layer than the C- and X-band radiation originates from ($\sim 1\text{--}2$ cm). As a result of this difference in vertical support, the phase and amplitude of T_{MERRA} estimates are likely not optimal for land surface inputs into soil moisture retrieval algorithms like LPRM. In order to better represent the vertical support of microwave-based LST, and therefore make better use of the MERRA dataset as input to LRPM, we test different scenarios in which the effective vertical support of MERRA predictions is increased.

The vertical distance between two measurements depths and the thermal properties of the medium determine the length of the time lag between soil temperature measurements at two different depths. Van Wijk and de Vries (1963) showed that a phase shift is accompanied by an exponential reduction in amplitude (A) and an increase in phase shift ($d\phi$) of the daily temperature cycle as the measurement depth is moved deeper into the soil Eqs. (4) and (5).

$$A_{z2} = A_{z1} e \left(\frac{dz}{z_d} \right) \quad (4)$$

The impact of land surface temperature on soil moisture anomaly detection

R. M. Parinussa et al.

Title Page

Abstract

Introduction

Conclusions

References

Tables

Figures

⏪

⏩

◀

▶

Back

Close

Full Screen / Esc

Printer-friendly Version

Interactive Discussion



$$d\varphi = \frac{-dz}{z_d} \quad (5)$$

where dz is the vertical distance ($z_2 - z_1$) and the damping depth (z_d) is an expression of the thermal properties of the medium. Holmes et al. (2011) demonstrated that by using only the measured phase shift between two temperature sets a time series of temperature data can be synchronised to estimate the temperature at a second depth according to Eqs. (4) and (5). Specifically, they found that a 3 h phase shift applied to the original MERRA product could estimate the temperature at 5 cm below the surface with a root mean square error (RMSE) of 1.8 K for a dense in situ network located in Oklahoma. For the present study a much smaller phase shift should be appropriate to estimate the temperature at ~ 1 –2 cm, but the exact value is difficult to estimate because it may depend on land cover and surface state. For this reason several different scenarios from the MERRA re-analysis LST dataset were evaluated for three different cases: (1) no phase lag (i.e. the original estimate), (2) a phase shift of 1/2 h and (3) a phase shift of 1 h. For a single pixel in Oklahoma (USA), Fig. 6 demonstrates the impact (time-lag and amplitude reduction) of these phase shift on MERRA LST estimates. In addition to the evaluated MERRA scenarios (original, 1/2 h and 1 h), a 2 and 3 h phase shift was included in Fig. 6 (for visualization purposes only), showing the damping in the amplitude and the associated time-lag as a result of the introduced phase shift. This figure also shows that the soil temperature profile is more vertically homogeneous at the Coriolis/WindSat overpass time (06:00 a.m./p.m. LST – local solar time) than at the Aqua/AMSR-E retrieval time (01.30 a.m./p.m.).

4 Results and discussion

4.1 Cross-verification

Soil moisture retrievals from the night-time (descending) AMSR-E observations are used for cross-verification of the outputs of the two evaluation techniques introduced

The impact of land surface temperature on soil moisture anomaly detection

R. M. Parinussa et al.

Title Page

Abstract

Introduction

Conclusions

References

Tables

Figures

◀

▶

◀

▶

Back

Close

Full Screen / Esc

Printer-friendly Version

Interactive Discussion



above (TC and R_{value}). Since the soil moisture data sets have been processed to have the same temporal mean and standard deviation, TC-based RMSE and R_{value} should contain essentially the same information (Entekhabi et al., 2010a) if both evaluation procedures are operating correctly. Figure 7 explores this issue in greater detail by showing a scatterplot between TC and the R_{value} results over the entire range of LPRM-derived canopy optical depths (τ) (see Fig. 2). Over this range ($0 < \tau < 1.10$) global RMSE acquired from the TC technique and global R_{value} results are selected and averaged within a series of $\tau = 0.01$ intervals, resulting in a set of 110 data pairs (Fig. 7). The coefficient of determination (R^2) between the two evaluation techniques was high ($R^2 = 0.78$). However, Fig. 7 does show deviations from the regression line in both the high and low extremes of the vegetation (class 1 and 6). The high mutual consistency between TC and R_{value} , which was shown in the other classes, breaks down at extreme vegetation levels due to a lack of variation in the R_{value} metric, suggesting that R_{value} may saturate at extreme vegetation amounts. Class 1 ($\tau < 0.10$) mainly represents desert areas with only few precipitation events. For this reason the R_{value} verification technique, which requires sampling across a large number of precipitation events, may lose sensitivity in very arid climate regions. On the other end of the scatterplot, class 6 (mainly rainforest areas), the deviation could be explained by the fact that the soil moisture signal becomes almost entirely masked due to the overlying canopy. When these two extreme vegetation regions are masked the coefficient of determination between the two evaluation techniques is strikingly high ($R^2 = 0.95$). This high level of consistency between the two techniques lends confidence to their interpretation as robust evaluation metrics.

4.2 Ka-band scenarios

As described in Sect. 3.2.1, T_{ka} retrievals were synthetically degraded using four different noise levels and then applied to generate a range of LPRM AMSR-E and Windsat-based soil moisture products. These products were then evaluated based on both the R_{value} and TC verification techniques. Results within the 6 vegetation optical depth

The impact of land surface temperature on soil moisture anomaly detection

R. M. Parinussa et al.

Title Page

Abstract

Introduction

Conclusions

References

Tables

Figures



Back

Close

Full Screen / Esc

Printer-friendly Version

Interactive Discussion



classes, as was shown in Fig. 3 (Table 1), were averaged resulting in Fig. 8. The left part of this figure shows results from the R_{value} technique, the right part shows results from the TC technique.

For both satellites (AMSR-E and Windsat) in both day- (ascending) and night-time (descending) retrievals, increasing the magnitude of the noise levels leads to a reduction in R_{value} for all vegetation density classes (Fig. 8, left panel). The figure also shows a steady decrease in R_{value} with increasing vegetation density which is consistent with expectations about the impact of vegetation density on the attenuation of microwave emission from the soil surface by the overlying canopy. As previously discussed (Sect. 4.1), this trend is broken for AMSR-E retrievals within class 1 (i.e. mainly desert areas) land cover conditions. For both satellites, the lowest R_{value} are found in class 6 where the LPRM does not typically report retrievals.

Figure 8 (right panel) shows comparable results for the TC method. In contrast with the R_{value} method, where an increasing value indicates a better soil moisture product, an increasing root mean square error (RMSE) indicates that the remotely sensed soil moisture product is of lower quality. For both satellites in both day- (ascending) and night-time (descending) retrievals the TC method confirms the findings of the R_{value} method. Increasing the artificial noise level on the T_{ka} inputs into LPRM leads to an increase in TC-estimated RMSE for subsequent LPRM soil moisture retrievals. Likewise, increasing vegetation density leads to a steady increase in TC-estimate RMSE for soil moisture retrievals. As was the case for R_{value} , the highest TC-estimated RMSE values are found for very densely-vegetated surfaces (i.e. class 6) which are typically masked in LPRM applications. This offers some confidence that TC can accurately identify areas of very poor retrieval accuracy. Finally, the similar response for both satellites with regards to variations in LST noise and vegetation density indicates that the lower spatial support of the WindSat sensor does not influence the results of the evaluation techniques.

Figure 8 also suggests that the LPRM has varying sensitivity to the surface temperature input under different vegetation conditions. Generally, the results of the evaluation

The impact of land surface temperature on soil moisture anomaly detection

R. M. Parinussa et al.

Title Page

Abstract

Introduction

Conclusions

References

Tables

Figures

⏪

⏩

◀

▶

Back

Close

Full Screen / Esc

Printer-friendly Version

Interactive Discussion

techniques for the different noise scenarios cluster in the extreme classes (1 and 6) suggesting a lower sensitivity of the LPRM to LST in these areas. In the other classes (2–5) the distribution for the different noise scenarios show a wider spread, indicating a higher sensitivity. Generally, this trend was confirmed by both verification techniques, although it is more profound in TC results.

Another important observations from Fig. 8, is that day-time observations from both satellites become of higher quality when the vegetation density increases compared to the night-time observations over the same areas. Several studies (Loew et al., 2011; Brocca et al., 2011) indicated this already, but none of them explained this phenomenon. One possible explanation is that the vegetation water content during the day decreases due to transpiration induced by photosynthesis, making the vegetation more transparent to microwave emission, and consequently increasing the sensitivity to the underlying soil moisture signal. Also, higher canopy temperatures during the day could lead to decreased vegetation optical depth values, resulting in the same higher penetration through the overlying canopy. In any case, these findings show that the traditional view, which expects a higher quality of night-time observations since the environmental state is closer to equilibrium at these times (de Jeu et al., 2008), might be incomplete.

4.3 MERRA scenarios

The TC and R_{value} evaluation techniques were also applied to the 3 different T_{MERRA} scenarios and results within the 6 vegetation classes (Table 1; Fig. 3) were averaged. Figure 9 show these results for both evaluation techniques, where the relative degradation (negative number; blue areas) or improvement (positive number; red areas) compared to the original retrieval strategy (LPRM using T_{Ka}) are plotted. Since the mutual consistency between both evaluation techniques was shown to break down at the high and low extremes of vegetation density (Sect. 4.1), only the results for vegetation classes 2 to 5 are presented here.

The impact of land surface temperature on soil moisture anomaly detection

R. M. Parinussa et al.

Title Page

Abstract

Introduction

Conclusions

References

Tables

Figures



Back

Close

Full Screen / Esc

Printer-friendly Version

Interactive Discussion

The impact of land surface temperature on soil moisture anomaly detection

R. M. Parinussa et al.

Title Page

Abstract

Introduction

Conclusions

References

Tables

Figures

⏪

⏩

◀

▶

Back

Close

Full Screen / Esc

Printer-friendly Version

Interactive Discussion



First, Fig. 9 is analyzed without differentiating results from the individual MERRA scenarios. Overall there is a trend between the relative performance of LPRM soil moisture retrievals using T_{MERRA} (versus T_{Ka}) and the vegetation density. In the lightly-vegetated classes (2 and 3), the performance of the soil moisture retrievals degrades when T_{MERRA} was used relative to T_{Ka} (majority is blue). However, the use of MERRA-based soil moisture retrievals actually improves LPRM soil moisture retrieval accuracy for class 4 and 5 (majority is red). A general consistency between the TC- and the R_{value} evaluation techniques is again apparent. There are some deviations between the performance of the two methods, but these are generally small (e.g. WindSat Ascending, class 2; AMSR-E Descending, class 3) or they are from observations taken under challenging conditions (AMSR-E Ascending; dense vegetation class 5). The relative impact of changing between T_{Ka} and T_{MERRA} tend to be larger for AMSR-E than for Windsat. This suggests that 01:30 a.m./p.m. (i.e. AMSR-E) observations are generally more sensitive to the transition from satellite observed LST to re-analysis LST than 06:00 a.m./p.m. (i.e. WindSat) observations.

Secondly, the impact of modifying the vertical support of T_{MERRA} estimates (via Eqs. 4 and 5) is analyzed. Generalizing these results is not straightforward since Fig. 9 shows a large variety of responses to this modification between the different satellites and their individual paths. AMSR-E day-time (ascending) observations deviate significantly when compared to the other analyses and generally show improved results with increasing phase shift. A 1 h phase shift shows the best results for AMSR-E day-time (ascending) observations, which could reflect an overestimation of the diurnal heating as shown previously in Holmes et al. (2011). Conversely, for AMSR-E night-time (descending) and WindSat (both paths) a 1/2 h phase shift in the T_{MERRA} dataset is optimal under low- to sparsely vegetated conditions (classes 2 and 3).

5 Conclusions and outlook

The results of this study show the impact of LST error on the anomaly detection skill of surface soil moisture retrievals derived from the Land Parameter Retrieval Model (LPRM). LPRM requires LST as an input and normally acquires this input from coincident Ka-band observations. In this study retrieved soil moisture from this default scenario is first compared to several scenarios where the Ka-band temperature input is synthetically degraded, and then to scenarios where LST is acquired from the MERRA re-analysis data. Two large-scale evaluation techniques, the R_{value} metric and the triple collocation (TC) method, both show sensitivity to resulting changes in soil moisture retrieval skill when the quality of the LST signal is synthetically degraded. Moreover, a strikingly high correlation ($R^2 = 0.95$) between the two evaluation techniques was demonstrated when extreme vegetation conditions were masked. This consistently lends credibility to results obtained from both metrics.

It was also shown that both evaluated LST products manifest themselves differently in the LPRM under different vegetation conditions. This finding may be related to the nature of MERRA and Ka-band LST estimates and how differences between the two estimates manifest themselves and/or interact under certain vegetation conditions. Ka-band LST is directly related to the true radiometric temperature of the land surface and is observed simultaneously to the other satellite observations while MERRA LST estimates are based on the use of a coupled land-atmospheric model to temporally smooth between assimilated observations of surface and atmospheric states. As a result, MERRA LST estimates tend to be temporally smoother than instantaneous Ka-band LST retrievals. Since vegetation also tends to reduce the (high frequency) temporal variation of LST, such conditions may be better suited for the application of MERRA-based LST than lightly-vegetated conditions. Likewise, MERRA LST estimates are likely of higher quality for dense vegetation cases since LST is tightly coupled to air temperature and presumably easier to estimate within an atmospheric

HESSD

8, 6683–6719, 2011

The impact of land surface temperature on soil moisture anomaly detection

R. M. Parinussa et al.

Title Page

Abstract

Introduction

Conclusions

References

Tables

Figures

⏪

⏩

◀

▶

Back

Close

Full Screen / Esc

Printer-friendly Version

Interactive Discussion

re-analysis system. These differences and their interaction result in favourable results for Ka-band LST estimates (relative to MERRA LST) for bare to sparsely vegetation cases (classes 2–3), however this tendency is reversed for the moderate and densely vegetation cases (classes 4–5). Consequently, the global impact of transitioning into MERRA-based LST product is relatively modest.

Since the MERRA LST estimates does not have the same vertical support as the Ka-band LST estimates we included two additional scenarios where a phase and amplitude adjustment of 1/2 and 1 h represented slightly deeper temperature levels. The response of this phase shift on the accuracy of LPRM soil moisture retrievals obtained from MERRA LST varies considerably between each case. However, Fig. 9 suggests that under sparsely vegetated conditions (class 2–3), introducing a 1/2 h phase shift generally outperforms the other MERRA scenarios. These results are based on the application of novel large-scale soil moisture evaluation techniques, and not on more traditional comparisons with ground-based soil moisture observations. Arguably, these two techniques are less reliable than more direct validation against ground-based soil moisture observations; however, the fact that key conclusions are supported by both TC and R_{value} results lends extra credence to their validity.

The results further suggest that AMSR (01:30 a.m./p.m.) observations are more sensitive to the transition from satellite observed LST to re-analysis LST than WindSat (06:00 a.m./p.m.) observations. This is an important finding, since the modern (SMOS) and future (SMAP) satellite both have similar overpass times (06:00 a.m./p.m.) as the WindSat satellite. The transition from C-band Windsat and AMSR-E results to L-band SMAP and SMOS is widely expected to yield improved surface soil moisture retrievals. However, Windsat and AMSR-E retain the advantage of a Ka-band for LST retrievals while SMAP and SMOS are (or will be) forced to estimate LST from ancillary data. Since, at least for some vegetation types, the use of this ancillary data appears associated with degradation in retrievals accuracy, a recommendation for future studies would be to include SMOS soil moisture retrievals to evaluate the magnitude of these LST degradations relative to the overall advantages associated with using lower frequency

The impact of land surface temperature on soil moisture anomaly detection

R. M. Parinussa et al.

[Title Page](#)[Abstract](#)[Introduction](#)[Conclusions](#)[References](#)[Tables](#)[Figures](#)[Back](#)[Close](#)[Full Screen / Esc](#)[Printer-friendly Version](#)[Interactive Discussion](#)

L-band radiometry to retrieve surface soil moisture. The work presented in this paper could be used as a framework for such evaluations.

Acknowledgements. This research was NASA-supported through Wade Crow's membership on the NASA SMAP mission science definition team.

References

Bisselink, B., van Meijgaard, E., Dolman, A., and de Jeu, R.: Initializing a regional climate model with satellite-derived soil moisture, *J. Geophys. Res.*, 116, D02121, doi:10.1029/2010JD014534, 2011.

Brocca, L., Melone, F., Moramarco, T., Wagner, W., Naeimi, V., Bartalis, Z., and Hasenauer, S.: Improving runoff prediction through the assimilation of the ASCAT soil moisture product, *Hydrol. Earth Syst. Sci.*, 14, 1881–1893, doi:10.5194/hess-14-1881-2010, 2010.

Brocca, L., Hasenauer, S., Lacava, T., Melone, F., Moramarco, T., Wagner, W., Dorigo, W., Matgen, P., Martinez-Fernandez, J., Llorens, P., Latron, J., Martin, C., and Bittelli, M.: Soil moisture estimation through ASCAT and AMSR-E sensors: An intercomparison and validation study across Europe, *Remote Sens. Environ.*, in revision, 2011.

Crow, W. and van den Berg, M.: An improved approach for estimating observation and model error parameters for soil moisture data assimilation, *Water Resources Research*, 46, W12519, doi:10.1029/2010WR009402, 2010b.

Crow, W. and Zhan, X.: Continental-Scale Evaluation of Remotely Sensed Soil Moisture Products, *IEEE Geosci. Remote Sens. Lett.*, 4, 451–455, 2007.

Crow, W., Miralles, D., and Cosh, M.: A Quasi-Global Evaluation System for Satellite-Based Surface Soil Moisture Retrievals. *IEEE T. Geosci. Remote*, 48, 2516–2527, 2010.

de Jeu, R. and Owe, M.: Further validation of a new methodology for surface moisture and vegetation optical depth retrieval, *Int. J. Remote Sens.*, 24, 4559–4578, 2003.

de Jeu, R., Wagner, W., Holmes, T., Dolman, A., van de Giesen, N., and Friesen, J.: Global Soil Moisture Patterns Observed by Space Borne Microwave Radiometers and Scatterometers, *Surv. Geophys.*, 29, 399–420, 2008.

Dorigo, W. A., Scipal, K., Parinussa, R. M., Liu, Y. Y., Wagner, W., de Jeu, R. A. M., and Naeimi, V.: Error characterisation of global active and passive microwave soil moisture datasets, *Hydrol. Earth Syst. Sci.*, 14, 2605–2616, doi:10.5194/hess-14-2605-2010, 2010.

The impact of land surface temperature on soil moisture anomaly detection

R. M. Parinussa et al.

Title Page

Abstract

Introduction

Conclusions

References

Tables

Figures



Back

Close

Full Screen / Esc

Printer-friendly Version

Interactive Discussion



The impact of land surface temperature on soil moisture anomaly detection

R. M. Parinussa et al.

Title Page

Abstract

Introduction

Conclusions

References

Tables

Figures

⏪

⏩

◀

▶

Back

Close

Full Screen / Esc

Printer-friendly Version

Interactive Discussion



- Draper, C., Walker, J., Steinle, P., de Jeu, R., and Holmes, T.: An Evaluation of AMSR-E Derived Soil Moisture over Australia, *Remote Sens. Environ.*, 113, 703–710, 2009.
- Entekhabi, D., Reichle, R., Koster, R., and Crow, W.: Performance Metrics for Soil Moisture Retrievals and Application Requirements, *J. Hydrometeorol.*, 11, 832–840, 2010a.
- 5 Entekhabi, D., Njoku, E., O'Neill, P., Kellogg, K., Crow, W., Edelstein, W., Entin, J., Goodman, S., Jackson, T., Johnson, J., Kimball, J., Piepmeier, J., Koster, R., McDonald, K., Moghadam, M., Moran, S., Reichle, R., Shi, J., Spencer, M., Thurman, S., Tsang, L., and van Zyl, J.: The Soil Moisture Active and Passive (SMAP) Mission, *Proc. IEEE*, 98, 704–716, 2010b.
- 10 Gaiser, P., St. Germain, K., Twarog, E., Poe, G., Purdy, W., Richardson, D., Grossman, W., Jones, W., Spencer, D., Golba, G., Cleveland, J., Choy, L., Bevilacqua, R., and Chang, P.: The WindSat Spaceborne Polarimetric Microwave Radiometer: Sensor Description and Early Orbit Performance, *IEEE T. Geosci. Remote*, 42, 2347–2360, 2004.
- Holmes, T., de Jeu, R., Owe, M., and Dolman, A.: Land surface temperature from Ka band passive microwave observations, *J. Geophys. Res.-Atmos.*, 114, D04113, doi:10.1029/2008JD010257, 2009.
- 15 Holmes, T., Jackson, J., Reichle, R., and Basara, J.: An Assessment of Surface Soil Temperature Products from Numerical Weather Prediction Models Using Ground-based Measurements, accepted, in revision, 2011.
- Huffman, G., Adler, R., Bolvin, D., Gu, G., Nelkin, E., Bowman, K., Hong, Y., Stocker, E., and Wolff, D.: The TRMM Multisatellite Precipitation Analysis (TMPA): Quasi-Global, Multi-
 20 year, Combined-Sensor Precipitation Estimates at Fine Scales, *J. Hydrometeorol.*, 8, 38–55, 2007.
- Jackson, T. and Schmugge, T.: Passive microwave remote sensing system for soil moisture: Some supporting research, *IEEE T. Geosci. Remote*, 27, 225–235, 1989.
- 25 Jackson, T., Hurkmans, R., Hsu, A., and Cosh, M.: Soil moisture algorithm validation using data from the Advanced Microwave Scanning Radiometer (AMSR-E) in Mongolia, *Rivista Italiana di Telerilevamento*, 30, 37–50, 2004.
- Jackson, T., Cosh, M., Bindlish, R., Starks, P., Bosch, D., Seyfried, M., Goodrich, D., Moran, M., and Du, J.: Validation of Advanced Microwave Scanning Radiometer Soil Moisture, *IEEE
 30 T. Geosci. Remote*, 48, 4256–4272, 2010.
- Kerr, Y., Waldteufel, P., Wigneron, J., Martinuzzi, J., Font, J., and Berger, M.: Soil moisture retrieval from space: The Soil Moisture and Ocean Salinity (SMOS) mission, *IEEE T. Geosci. Remote*, 39, 1729–1735, 2001.

The impact of land surface temperature on soil moisture anomaly detection

R. M. Parinussa et al.

Title Page

Abstract

Introduction

Conclusions

References

Tables

Figures

⏪

⏩

◀

▶

Back

Close

Full Screen / Esc

Printer-friendly Version

Interactive Discussion



- Koster, R., Schubert, S., and Suarez, M.: Analyzing the concurrence of meteorological droughts and warm periods, with implications for the determination of evaporative regime, *J. Climate*, 22, 3331–3341, 2009.
- Li, L., Njoku, E., Im, E., Chang, P., and Germaine, K.: A preliminary survey of radio-frequency interference over the U.S. in Aqua AMSR-E data, *IEEE T. Geosci. Remote*, 42, 380–390, 2004.
- Li, L., Gaiser, W., Gao, B., Bevilacqua, R., Jackson, T., Njoku, E., Rudiger, C., Calvet, J., and Bindlish, R.: WindSat Global Soil Moisture Retrieval and Validation, *IEEE T. Geosci. Remote*, 48, 2224–2241, 2010.
- Loew, A. and Schlenz, F.: A dynamic approach for evaluating coarse scale satellite soil moisture products, *Hydrol. Earth Syst. Sci.*, 15, 75–90, doi:10.5194/hess-15-75-2011, 2011.
- Loew, A., Holmes, T., and de Jeu, R.: The European heat wave 2003: Early indicators from multisensoral microwave remote sensing?, *J. Geophys. Res.*, 114, D05103, doi:10.1029/2008JD010533, 2009.
- Meesters, A., de Jeu, R., and Owe, M.: Analytical derivation of the vegetation optical depth from the microwave polarization difference index, *IEEE Geosci. Remote Sens. Lett.*, 2, 121–123, 2005.
- Miralles, D., Crow, W., and Cosh, M.: Estimating Spatial Sampling Errors in Coarse-Scale Soil Moisture Estimates Derived from Point-Scale Observations, *J. Hydrometeorol.*, 11, 1423–1429, 2010.
- Miralles, D. G., Holmes, T. R. H., De Jeu, R. A. M., Gash, J. H., Meesters, A. G. C. A., and Dolman, A. J.: Global land-surface evaporation estimated from satellite-based observations, *Hydrol. Earth Syst. Sci.*, 15, 453–469, doi:10.5194/hess-15-453-2011, 2011.
- Naeimi, V., Scipal, K., Bartalis, Z., Hasenauer, S., and Wagner, W.: An Improved Soil Moisture Retrieval Algorithm for ERS and METOP Scatterometer Observations, *IEEE T. Geosci. Remote Sens.*, 47, 1999–2013, 2009.
- NSIDC – National Snow and Ice Data Centre: Data products and services, Boulder, Colo, 2006.
- Owe, M., de Jeu, R., and Holmes, T.: Multisensor historical climatology of satellite-derived global land surface moisture, *J. of Geophys. Res.-Earth*, 113, F01002, doi:10.1029/2007JF000769, 2008.
- Parinussa, R., Holmes, T., and de Jeu, R.: Soil moisture retrievals from the WindSat spaceborne polarimetric microwave radiometer, *IEEE T. Geosci. Remote Sens.*, in revision, 2011.

The impact of land surface temperature on soil moisture anomaly detection

R. M. Parinussa et al.

Title Page

Abstract

Introduction

Conclusions

References

Tables

Figures

⏪

⏩

◀

▶

Back

Close

Full Screen / Esc

Printer-friendly Version

Interactive Discussion



Reichle, R., Koster, R., Liu, P., Mahanama, S., Njoku, E., and Owe, M.: Comparison and assimilation of global soil moisture retrievals from the Advanced Microwave Scanning Radiometer for the Earth Observing System (AMSR-E) and the Scanning Multichannel Microwave Radiometer (SMMR), *J. Geophys. Res.*, 112, D09108, doi:10.1029/2006JD008033, 2007.

5 Rienecker, M., Suarez, M., Gelaro, R., Todling, R., Bacmeister, J., Liu, E., Bosilovich, M., Schubert, S., Takacs, L., Kim, G., Bloom, S., Chen, J., Collins, D., Conaty, A., da Silva, A., Gu, W., Joiner, J., Koster, R., Lucchesi, R., Molod, A., Owe, T., Pawson, S., Pegion, P., Redder, C., Reichle, R., Robertson, F., Ruddick, A., Sienkiewicz, M. and Woollen, J.: MERRA – NASA’s Modern-Era Retrospective Analysis for Research and Applications, <http://gmao.gsfc.nasa.gov/pubs/docs/Rienecker443.pdf>, last access: July 2011, *J. Climate*, submitted, 2011.

Scipal, K., Holmes, T., de Jeu, R., Naeimi, V., and Wagner, W.: A possible solution for the problem of estimating the error structure of global soil moisture data sets, *Geophys. Res. Lett.*, 35, L24403, doi:10.1029/2008GL035599, 2008.

15 van Wijk, W. and de Vries, D.: Periodic temperature variations in a homogeneous soil, *Phys. Plant Environ*, North-Holland Publ. Co., Amsterdam, 102–143, 1963.

Wagner, W., Naeimi, V., Scipal, K., de Jeu, R., and Martinez-Fernandez, J.: Soil moisture from operational meteorological satellites, *Hydrogeol. J.*, 15, 121–131, 2007.

The impact of land surface temperature on soil moisture anomaly detection

R. M. Parinussa et al.

Table 1. Boundaries to select different vegetation optical depth (τ) classes.

Class	Boundaries
1	$\tau < 0.1$
2	$0.1 \leq \tau < 0.3$
3	$0.3 \leq \tau < 0.5$
4	$0.5 \leq \tau < 0.7$
5	$0.7 \leq \tau < 0.9$
6	$\tau \geq 0.9$

Title Page

Abstract

Introduction

Conclusions

References

Tables

Figures

I◀

▶I

◀

▶

Back

Close

Full Screen / Esc

Printer-friendly Version

Interactive Discussion

The impact of land surface temperature on soil moisture anomaly detection

R. M. Parinussa et al.

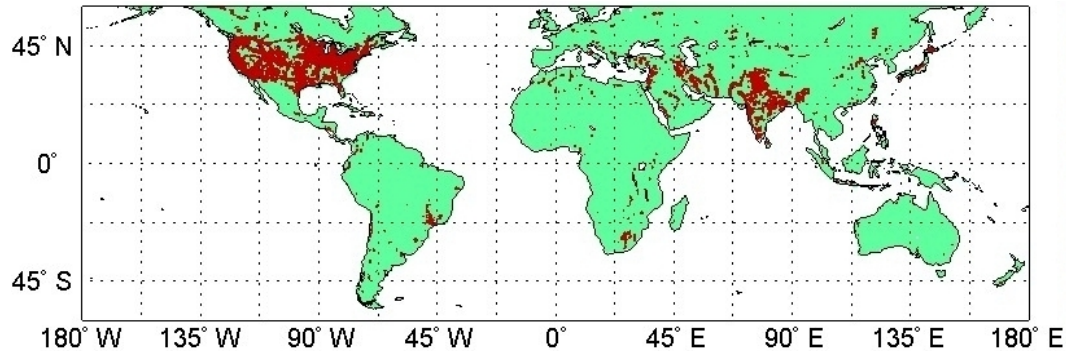


Fig. 1. The green areas indicate the areas where C-band observations are used. The red areas indicate where C-band observations are contaminated by RFI and X-band observations are used.

[Title Page](#)[Abstract](#)[Introduction](#)[Conclusions](#)[References](#)[Tables](#)[Figures](#)[⏪](#)[⏩](#)[◀](#)[▶](#)[Back](#)[Close](#)[Full Screen / Esc](#)[Printer-friendly Version](#)[Interactive Discussion](#)

The impact of land surface temperature on soil moisture anomaly detection

R. M. Parinussa et al.

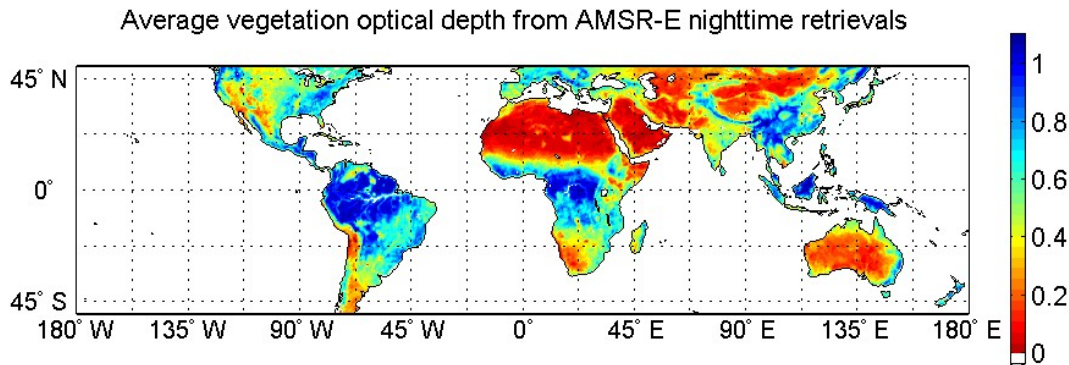


Fig. 2. Average vegetation optical depth (τ) for the AMSR-E descending overpass retrieved in the period February 2003 till December 2010.

[Title Page](#)[Abstract](#)[Introduction](#)[Conclusions](#)[References](#)[Tables](#)[Figures](#)[◀](#)[▶](#)[◀](#)[▶](#)[Back](#)[Close](#)[Full Screen / Esc](#)[Printer-friendly Version](#)[Interactive Discussion](#)

The impact of land surface temperature on soil moisture anomaly detection

R. M. Parinussa et al.

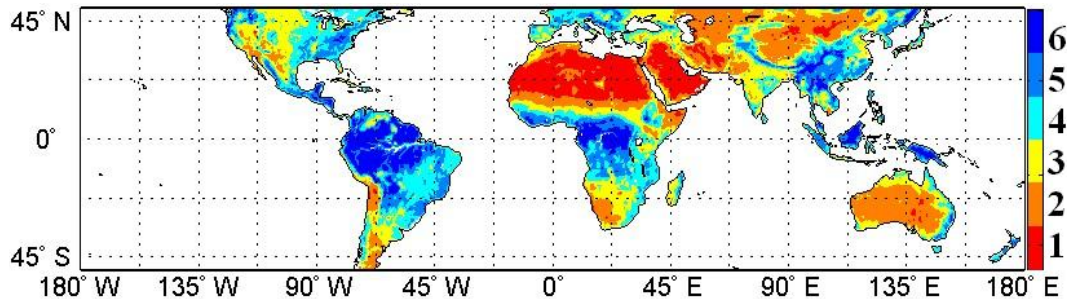


Fig. 3. Vegetation classes over which the R_{value} method and the TC method were evaluated based on the simultaneously derived average vegetation optical depth (τ) of the AMSR-E descending overpass for the period February 2003 till December 2010.

[Title Page](#)[Abstract](#)[Introduction](#)[Conclusions](#)[References](#)[Tables](#)[Figures](#)[⏪](#)[⏩](#)[◀](#)[▶](#)[Back](#)[Close](#)[Full Screen / Esc](#)[Printer-friendly Version](#)[Interactive Discussion](#)

The impact of land surface temperature on soil moisture anomaly detection

R. M. Parinussa et al.

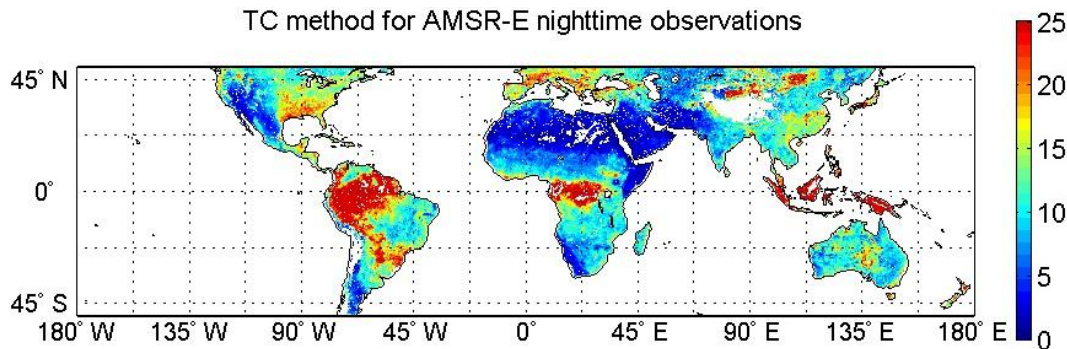


Fig. 5. Example of the TC method for the AMSR-E descending overpass, the analysis period was January 2007 till September 2010.

[Title Page](#)[Abstract](#)[Introduction](#)[Conclusions](#)[References](#)[Tables](#)[Figures](#)[⏪](#)[⏩](#)[◀](#)[▶](#)[Back](#)[Close](#)[Full Screen / Esc](#)[Printer-friendly Version](#)[Interactive Discussion](#)

The impact of land surface temperature on soil moisture anomaly detection

R. M. Parinussa et al.

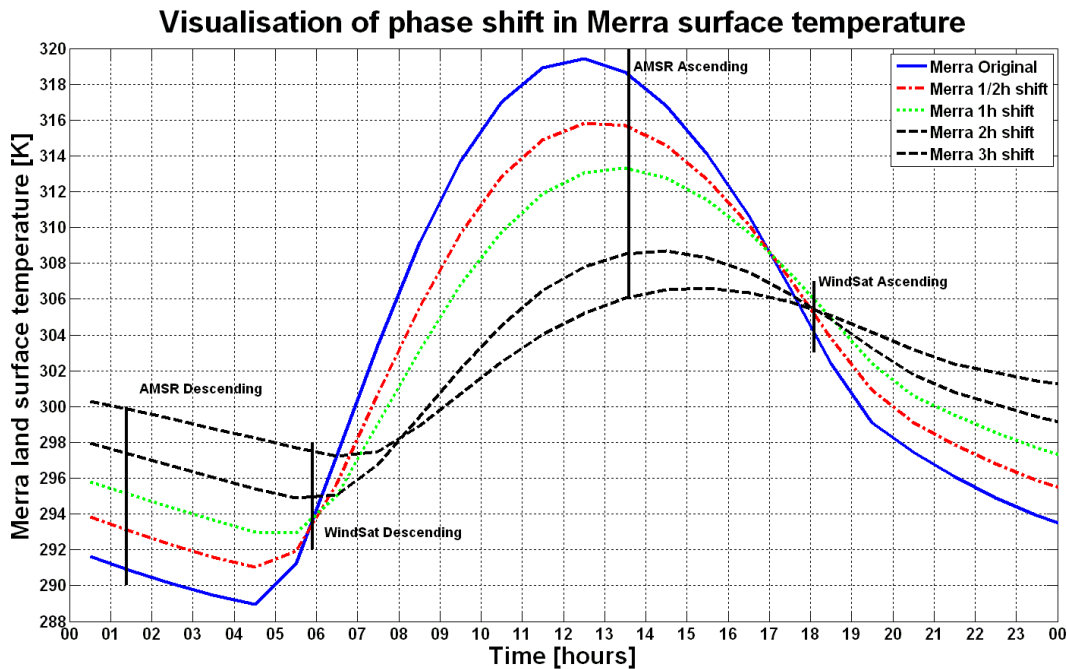


Fig. 6. Detailed diurnal land surface temperature time series from MERRA for 1 July 2009 in Oklahoma, United States of America.

Discussion Paper | Discussion Paper | Discussion Paper | Discussion Paper | Discussion Paper

Title Page

Abstract Introduction

Conclusions References

Tables Figures

⏪ ⏩

◀ ▶

Back Close

Full Screen / Esc

Printer-friendly Version

Interactive Discussion



The impact of land surface temperature on soil moisture anomaly detection

R. M. Parinussa et al.

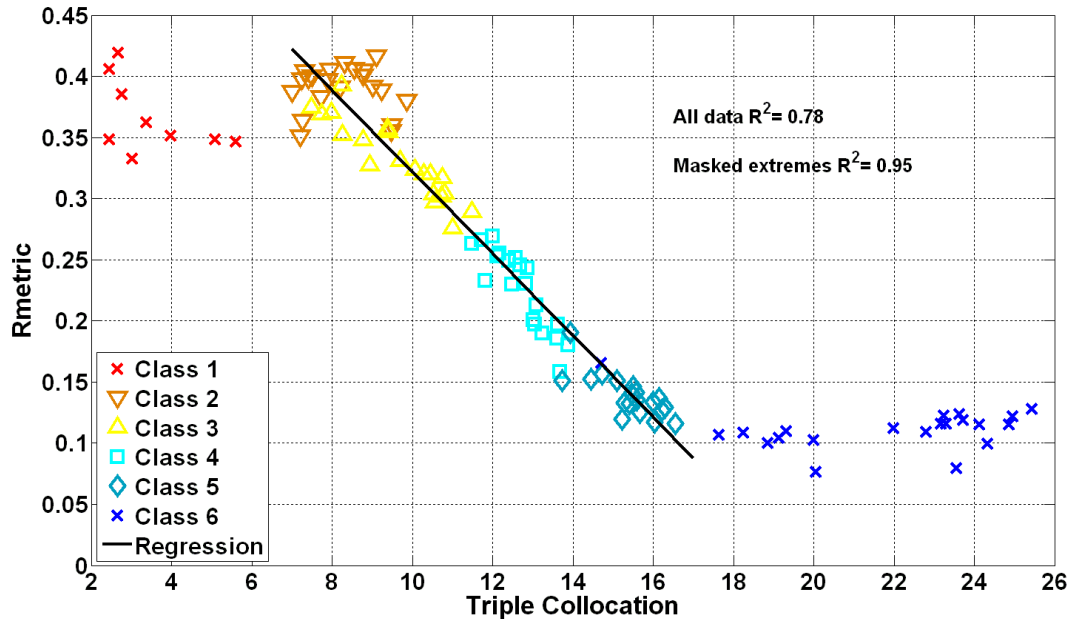


Fig. 7. Scatterplot between the TC and the R_{value} results for AMSR-E night-time (descending) retrievals. Classes refer to ranges of canopy optical depth defined in Table 1.

Title Page

Abstract

Introduction

Conclusions

References

Tables

Figures

◀

▶

◀

▶

Back

Close

Full Screen / Esc

Printer-friendly Version

Interactive Discussion

The impact of land surface temperature on soil moisture anomaly detection

R. M. Parinussa et al.

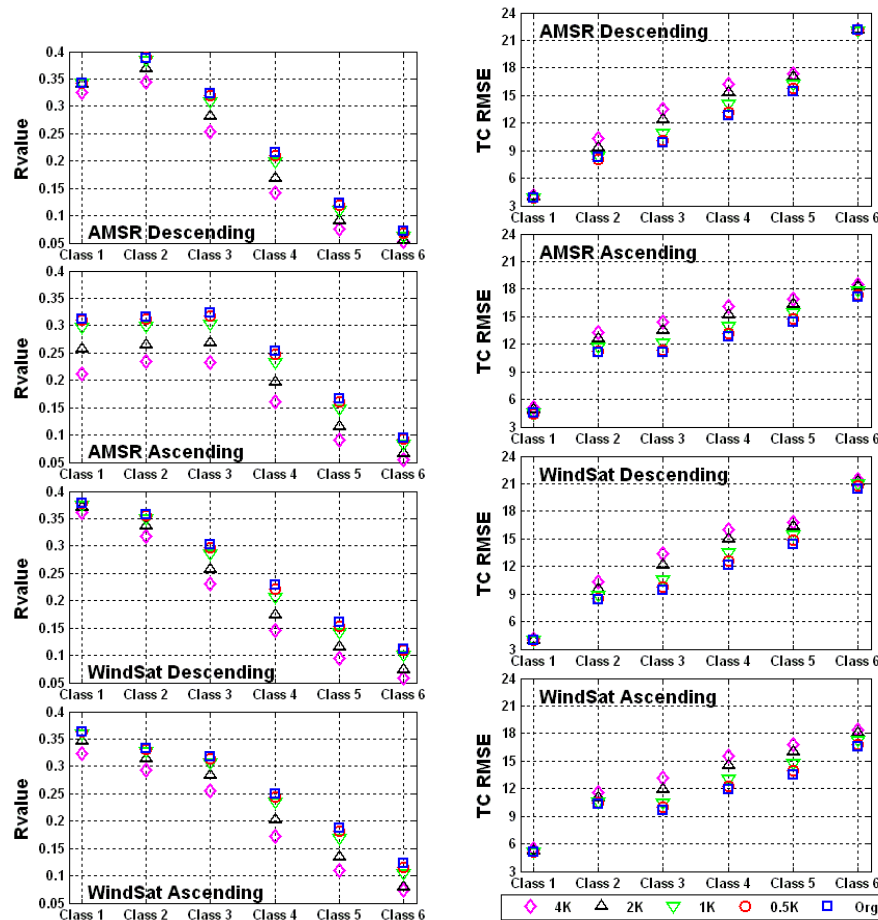


Fig. 8. Results of the R_{value} and the TC method for AMSR-E and WindSat with their day (ascending) and night-time (descending) observations separated after synthetic degradation of T_{Ka} . Symbols represent different levels of artificial Gaussian noise applied during the degradation step.

Title Page

Abstract

Introduction

Conclusions

References

Tables

Figures

◀

▶

◀

▶

Back

Close

Full Screen / Esc

Printer-friendly Version

Interactive Discussion

The impact of land surface temperature on soil moisture anomaly detection

R. M. Parinussa et al.

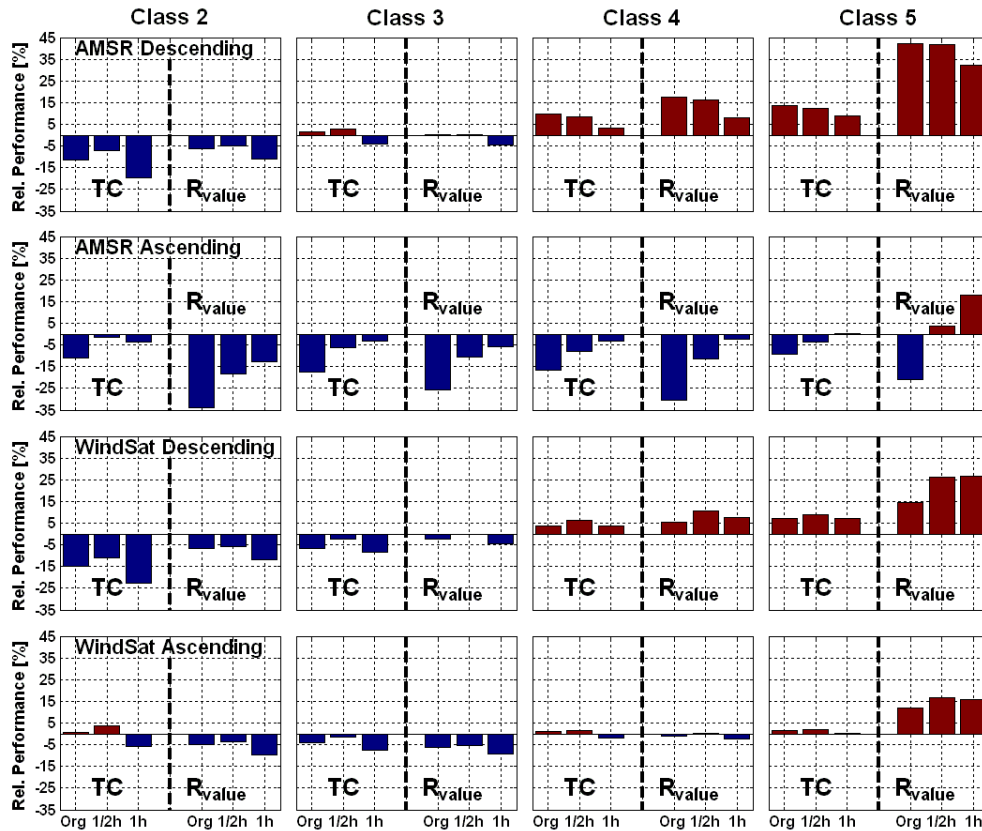


Fig. 9. Results of the TC and R_{value} method for AMSR-E and WindSat with their day- (ascending) and night-time (descending) observations separated for the T_{MERRA} scenarios. The x-axis represents the different MERRA scenarios. The y-axis captures change relative to the baseline case (T_{Ka}). Improvement relative to this baseline is reflected in positive values shaded in red and degradation in negative values shaded in blue.

Title Page

Abstract Introduction

Conclusions References

Tables Figures

⏪ ⏩

◀ ▶

Back Close

Full Screen / Esc

Printer-friendly Version

Interactive Discussion

